

## Design of a cementitious material with nopal mucilage and PET aggregates to improve the electrochemical properties of reinforced concrete.

E. C. Menchaca-Campos<sup>1</sup> , Y. Díaz-Blanco<sup>2\*</sup> , C. I. Rocabrundo-Valdes<sup>1</sup> ,  
Y. Tamayo-Aguilar<sup>3</sup> , A. Flores-Nicolas<sup>4</sup> , J. Uruchurtu-Chavarín<sup>1</sup> 

\*Contact author: [yohadiaz12@gmail.com](mailto:yohadiaz12@gmail.com)

DOI: <https://doi.org/10.21041/ra.v16i2.1012>

Received: 11/01/2026 | Received in revised form: 05/04/2026 | Accepted: 07/04/2026 | Published: 01/05/2026

### ABSTRACT

This work focused on the study of reinforced concrete (RC) with the addition of nopal mucilage (NM) and (polyethylene terephthalate) PET aggregates. Samples were prepared with different PET geometries: particles (P), a mixture of long fibers and particles (LF-P), and short fibers (SF) combined with NM. Samples were evaluated using half-cell potential (HCP), electrochemical noise (EN), and linear polarization resistance (LPR). A decrease in compressive strength ( $f_c$ ) values was observed with increasing PET percentage. Samples with PET and NM achieved lower values of corrosion rate ( $I_{corr}$ ). PET design and storing the NM can be a challenge to analyze. Both materials contributed to increase the durability of RC.

**Keywords:** reinforcing concrete, PET, nopal mucilage, corrosion, electrochemical techniques.

**Cite as:** Menchaca-Campos, E. C., Díaz-Blanco, Y., Rocabrundo-Valdes, C. I., Tamayo-Aguilar, Y., Flores-Nicolas, A., Uruchurtu-Chavarín, J. (2026), “*Design of a cementitious material with nopal mucilage and PET aggregates to improve the electrochemical properties of reinforced concrete.*”, Revista ALCONPAT, 16 (2), pp. 202 – 222, DOI: <https://doi.org/10.21041/ra.v16i2.1012>.

<sup>1</sup> Centro de Investigación en Ingeniería y Ciencias Aplicadas. Universidad Autónoma del Estado de Morelos. Av. Universidad No. 1001, Col Chamilpa, Cuernavaca, Morelos, México. C.P. 62210.

<sup>2</sup> Posdoc. SECIHTI. Centro de Investigación en Ingeniería y Ciencias Aplicadas. Universidad Autónoma del Estado de Morelos. Av. Universidad No. 1001, Col Chamilpa, Cuernavaca, Morelos, México. C.P. 62210.

<sup>3</sup> Posdoc. SECIHTI. Posgrado en Ciencias Agropecuarias. Facultad de Ciencias Agropecuarias. Universidad Autónoma del Estado de Morelos. Av. Universidad No. 1001, Col Chamilpa, Cuernavaca, Morelos, México. C.P. 62210.

<sup>4</sup> Facultad de Ingeniería, Arquitectura y Diseño, Universidad Autónoma de Baja California, Carretera Transpeninsular Ensenada-Tijuana, 3917, Playitas, 22860, Ensenada, B.C. México.

### Contribution of each author

In this work, the original idea of the research was by Y. Díaz-Blanco Yohandry (30%), C. Menchaca-Campos (40%) and J. Uruchurtu-Chavarín (40%). The administration of the project oversaw C. Menchaca-Campos (60%) and J. Uruchurtu-Chavarín (40%). The methodology and experimentation oversaw Y. Díaz-Blanco (50%), C. I. Rocabrundo-Valdés (30%), C. Menchaca-Campos (10%) and J. Uruchurtu-Chavarín (10%). The data processing was carried out by Y. Díaz-Blanco (40%), C. I. Rocabrundo-Valdés (20%), Y. Tamayo-Aguilar (20%), A. Flores-Nicolas (20%). The writing, revision and edition oversaw Y. Díaz-Blanco (20%), C. Menchaca-Campos (20%), C. I. Rocabrundo-Valdés (20%), Y. Tamayo-Aguilar (15%), A. Flores-Nicolas (15%), J. Uruchurtu-Chavarín (10%). The analysis and discussion of results was by Y. Díaz-Blanco (30%), C. Menchaca-Campos (20%), C. I. Rocabrundo-Valdés (20%), A. Flores-Nicolas (10%), J. Uruchurtu-Chavarín (20%).

### Creative Commons License

Copyright 2026 by the authors. This work is an Open-Access article published under the terms and conditions of an International Creative Commons Attribution 4.0 International License ([CC BY 4.0](https://creativecommons.org/licenses/by/4.0/)).

## Design of a cementitious material with nopal mucilage and PET aggregates to improve the electrochemical properties of reinforced concrete.

### ABSTRACT

This work focused on the study of reinforced concrete (RC) with the addition of nopal mucilage (NM) and (polyethylene terephthalate) PET aggregates. Samples were prepared with different PET geometries: particles (P), a mixture of long fibers and particles (LF-P), and short fibers (SF) combined with NM. Samples were evaluated using half-cell potential (HCP), electrochemical noise (EN), and linear polarization resistance (LPR). A decrease in compressive strength ( $f_c$ ) values was observed with increasing PET percentage. Samples with PET and NM achieved lower values of corrosion rate ( $I_{corr}$ ). PET design and storing the NM can be a challenge to analyze. Both materials contributed to increased the durability of RC.

**Keywords:** reinforcing concrete, PET, nopal mucilage, corrosion, electrochemical techniques.

## Projeto de um material cimentício com mucilagem nopal e agregados PET para melhorar as propriedades eletroquímicas do concreto armado.

### RESUMO

Este trabalho teve como foco o estudo do concreto armado (RC) com adição de mucilagem de nopal (NM) e agregados de tereftalato de polietileno (PET). Foram preparadas amostras com diferentes geometrias de PET: partículas (P), mistura de fibras longas e partículas (LF-P) e fibras curtas (SF), combinadas com NM. As amostras foram avaliadas por meio de potencial de meia-célula (HCP), ruído eletroquímico (EN) e resistência à polarização linear (LPR). Os valores de resistência à compressão ( $f_c$ ) diminuíram com a adição de PET. As amostras com PET e NM apresentaram menores valores de velocidade de corrosão ( $I_{corr}$ ). A configuração geométrica do PET e o armazenamento da NM podem representar desafios analíticos. Ambos os materiais contribuíram para aumentar a durabilidade do concreto armado.

**Palavras-chave:** concreto armado, PET, mucilagem de nopal, corrosão, técnicas eletroquímicas.

### Discussions and subsequent corrections to the publication

Any dispute, including the replies of the authors, will be published in the first issue of 2027 provided that the information is received before the closing of the third issue of 2026.

### Legal Information

Revista ALCONPAT is a quarterly publication by the Asociación Latinoamericana de Control de Calidad, Patología y Recuperación de la Construcción, Internacional, A.C., Km. 6 antigua carretera a Progreso, Mérida, Yucatán, 97310, Tel. +52 1 983 419 8241, [alconpat.int@gmail.com](mailto:alconpat.int@gmail.com), Website: [www.alconpat.org](http://www.alconpat.org)

Reservation of rights for exclusive use No.04-2013-011717330300-203, and ISSN 2007-6835, both granted by the Instituto Nacional de Derecho de Autor. Responsible editor: Pedro Castro Borges, Ph.D. Responsible for the last update of this issue, Informatics Unit ALCONPAT, Elizabeth Sabido Maldonado.

The views of the authors do not necessarily reflect the position of the editor.

The total or partial reproduction of the contents and images of the publication is carried out in accordance with the COPE code and the CC BY 4.0 license of the Revista ALCONPAT.

## NOMENCLATURE

Concept	Abbreviation
Reinforced concrete	RC.
Nopal mucilage	NM.
Polyethylene terephthalate	PET.
Particles	P.
Long fibers and particles	LF-P.
Short fibers	SF.
Half-cell potential	HCP.
Electrochemical noise	EN.
Linear polarization resistance	LPR.
Compressive strength	$f'_c$ .
Corrosion rate	$I_{corr}$ .
Acero de refuerzo	RS.
Reinforcing steel	CI.
Polarization resistance	$R_p$ .
Concrete reinforcing steel	CRS.
Corrosion potential	$E_{corr}$ .
Electrochemical noise resistance	$R_n$ .

### 1. INTRODUCTION

Nowadays, the concrete durability is one of the most important properties to consider for design of reinforced concrete structures. There are various internal and external factors that affect the concrete durability, such as: i) quality of materials used in the mix, type of reinforcement, water/cement ratio; as well as ii) exposure conditions to which the structures will be subjected during their useful life (Valipour, Shekarchi, and Ghods 2014).

Within the concrete matrix, the reinforcing steel (RS) is capable of developing a passive layer of ferric oxide (electrochemical barrier) (Ben Harb et al. 2020), that keeps it protected while maintaining the high alkalinity conditions of cement paste, in the absence of external aggressive agents that may corrode the steel surface (Abdel-Gaber, Khamis, and Hefnawy 2011). Likewise, the concrete cover offers physical protection to the reinforcement of the surrounding environment. In marine environments, chloride-induced corrosion is one of the main causes of deterioration of RS. In general, these ions can enter to concrete from the environment and diffuse through the concrete pore network (Abd El Fattah et al. 2018), or they can be present in the mix materials such as: fine and coarse aggregates (Saricimen et al. 2002). Inside the concrete, these ions can reach the metal surface and cause pitting corrosion (Abd El Fattah et al. 2018). In this sense, numerous investigations have focused on the study of concrete corrosion caused by chloride ions. (Andrade, Alonso, and Sarría 2002).

In order to extend the useful life of structures, various authors have focused on the study of reinforced concrete durability. (Gartner, Kosec, and Legat 2016; Pan et al. 2020). Several methods are reported in the literature to prevent and counteract the corrosion of RC, such as the following: cathodic protection (Gartner et al. 2016), coatings (Lee et al. 2018), admixed corrosion inhibitors (Ben Harb et al. 2020; Palanisamy et al. 2018; De Schutter and Luo 2004), surface applied corrosion inhibitors (Gartner et al. 2016; Monticelli 2018), supplementary cementitious materials (Pan et al. 2020), polymer aggregates in mixtures (Díaz-Blanco et al. 2019), among others.

Among the methods described above, the use of corrosion inhibitors (CI) has proven to be the most accepted and widely used, due to their low cost and easy application. (Umoren et al. 2019). Some of these inhibitors such as nitrite-based compounds (Garcés et al. 2008; Okeniyi, Loto, and Popoola 2015), chromates and dichromates (Okeniyi, Loto, and Popoola 2015; Qian and Cusson 2004) are classified as inorganic inhibitors and have a high inhibitory effect (Umoren et al. 2019). On the other hand, they have a significant disadvantage associated with the high toxicity presented, becoming harmful to human health (RAJA, GHOREISHIAMIRI, and ISMAIL 2015).

More recent is the use of natural inhibitors added to concrete to mitigate corrosion due to chloride ions. (Loto et al. 2013). These inhibitors are becoming more and more relevant, mainly due to their availability in nature, low cost and because they are more environmental friendly (Ormellese et al. 2006).

In this sense, NM presents itself as an excellent alternative to solve the problem of deterioration of reinforced concrete structures in marine environments and corrosion pathologies in RC, in the search for alternatives and new materials for construction.

Some authors have studied the effect of inhibitors on the electrochemical behavior of RS. Palanisamy et al. (Palanisamy et al. 2018) investigated the powdered extract of *ricinus communis* fruit as a CI in concrete samples exposed to a 3.5% NaCl solution. The results showed a remarkable inhibitory effect after 120 days of exposure, due to the formation of a passive film on the steel surface. From the electrochemical parameters of the Nyquist diagram and polarization curves, they obtained an inhibitor efficiency of 87% and 79%. The concrete samples exhibited an increase in compressive strength with increasing inhibitor concentration.

Pradipta et al. (Pradipta, Kong, and Tan 2019) compared the effect of a natural inhibitor from a green tea leaf extract with a commercial calcium nitrite inhibitor according to concentration and volume. The results indicated that at the same inhibitor concentration the CR was very similar. At the same volume there was a significant increase in the CR for the samples with calcium nitrite inhibitor, with values higher than 150  $\mu\text{m}$  / year after 12 wetting-drying cycles. On the contrary, the CR for the samples with green tea inhibitor remained around 40  $\mu\text{m}$ /year. The polarization resistance ( $R_p$ ) was superior for the green tea inhibitor compared to the calcium nitrite inhibitor throughout the exposure period.

Loto et al. (Loto et al. 2013) studied *vernonia amygdalina* leaf extract as a CI of mild steel in RC. Four inhibitor concentrations of 25, 50, 75 and 100% were obtained in distilled water. The results show an efficiency of 90.08% for the concrete sample with 25% of *vernonia amygdalina* extract. The potential values were more noble (less negative) for the same concentration of 25% compared to the rest of the samples. The authors conclude that *vernonia amygdalin* extract is a good CI of mild steel embedded in concrete exposed to a 3.5% sodium chloride solution.

Other natural extracts from plants have been used as CI in the concrete reinforcing steel (CRS) such as: *morinda lucida* (Okeniyi, Loto, and Idowu Popoola 2015), ginger (Liu et al. 2019), *rhizophora mangle L* (Okeniyi, Loto, and Popoola 2015), *olive leaves* (Ben Harb et al. 2020), *prosopis juliflora* (Palanisamy et al. 2016), maize gluten meals (Zhang, Ba, and Wu 2019), algae gel (Xu et al. 2015), NM (Díaz Blanco et al. 2019; Martinez-Molina et al. 2016), among others.

To improve concrete durability as well as other properties, there are many materials that have been added to concrete mixes in different sizes, percentages and geometries. This is the case for some synthetic waste materials, especially polyethylene terephthalate (PET) from post-consumer beverage bottles (Foti 2019).

Due to its diverse properties, PET has been studied for its potential use within a concrete matrix, primarily to modify its mechanical properties, among others. On the other hand, the study of the corrosion pathology of RC with PET, especially in marine environments is more recent and can become an excellent alternative to solve this problem.

In recent years, the problem related to environmental pollution has been the subject of study of great interest, which is why the recycling of some polymers for their subsequent use in concrete has been increasingly relevant. Some properties of PET make it very attractive as an aggregate in the concrete, for example: water and chemicals resistance, impact resistance, light weight, stability to atmospheric conditions, and acts as a barrier for gases and liquids, such and as stated by other authors (Díaz-Blanco et al. 2019; Siddique, Khatib, and Kaur 2008).

Many authors have studied the effect of different PET geometries on concrete properties with two main applications: i) to improve mechanical properties and ii) to improve durability (Ongpeng et al. 2020). In this sense, the following properties of concrete have been investigated, such as: workability of the mixture (Alfahdawi et al. 2019; Rahmani et al. 2013; Sadrumontazi et al. 2015; Saikia and De Brito 2014), compressive and flexural strength (Adnan and Dawood 2020; Alfahdawi et al. 2019; Borg, Baldacchino, and Ferrara 2016; Rahmani et al. 2013), porosity (Alfahdawi et al. 2019; Sadrumontazi et al. 2015), water absorption and electrical resistance (Sadrumontazi et al. 2015), cracking resistance (Adnan and Dawood 2020; Sadrumontazi et al. 2015), chloride penetration (Won et al. 2010) and corrosion resistance (Díaz-Blanco et al. 2019). Many of these studies involve PET fibers with a few centimeters of length (Adnan and Dawood 2020; Alfahdawi et al. 2019; Borg et al. 2016; Thomas and Moosvi 2020; Won et al. 2010), pellets (Saikia and De Brito 2014) and particles with some millimeters of wide and length (Adnan and Dawood 2020; Noroozi et al. 2019; Rahmani et al. 2013; Sadrumontazi et al. 2015; Saikia and De Brito 2014).

Saikia y Brito (Saikia and De Brito 2014) investigated the effect of recycled PET particles on the concrete properties in the fresh and hardened state. In this study, the coarse and fine aggregate was replaced by 5, 10 and 15% by three types of PET particles in a volume/volume ratio. The results indicate a reduction in the settlement of the mix with the larger PET and the smaller PET aggregates. On the contrary, an improvement of this property was reported for the mixture with modified PET aggregates. The density and compressive and flexural strength of all the samples with PET aggregates decrease with the increase in percentage of PET. On the other hand, the authors observed an improvement in abrasion resistance with the use of different types of PET.

Won et al. (Won et al. 2010) analyzed the behavior of recycled PET fiber-reinforced cement composite in terms of durability for different aggressive media. The chloride permeability results were very similar for the recycled PET fiber-reinforced cement composite samples and the control sample. The highest compressive strength values were maintained around 28 MPa at 30, 60, 90 and 120 days for the samples exposed to saline and calcium chloride solutions. On the other hand, the fibers surface suffered a greater deterioration when the recycled PET fiber-reinforced cement composite was exposed to the alkaline environment. The deterioration of the fibers was intermediate in the sulfuric acid environment and were low in the other three aggressive solutions. Díaz-Blanco et al. (Díaz-Blanco et al. 2019) determined some electrochemical parameters of the CRS with the addition of PET in form of fibers and rectangles particles with a substitution percentage of 3, 5 and 8% respect to volume of the sand. For the concrete with PET aggregates, more noble corrosion potential ( $E_{\text{corr}}$ ) values ( $> -250$  mV) were obtained, compared to the control sample which maintained more negative values ( $< -250$  mV). The electrochemical resistance noise ( $R_n$ ) and  $R_p$  values for the samples with rectangles particles and mixture of fibers-rectangles of PET was higher than  $2 \times 10^5 \Omega \cdot \text{cm}^2$ , whereas the samples with fibers showed a slightly higher behavior than the control sample with values between  $4 \times 10^4$  and  $1.5 \times 10^5 \Omega \cdot \text{cm}^2$  respectively. The authors conclude that there is a relationship between the geometry, size and percentage of PET and the electrochemical properties of CRS.

Silva et al. (Silva, de Brito, and Saikia 2013) studied the influence of curing conditions of concrete with PET aggregates in terms of its mechanical and durability properties. The authors used three types of PET with two substitution percentages of 7.5 and 15% as replacement of fine and coarse

aggregate. The samples exposed to the wet chamber showed the highest values of compression strength, although the resistance decreased with the increase in PET percentage. The concrete with plastic aggregates showed in general a better behavior against drying shrinkage, especially in the more humid environment. On the other hand, the chloride diffusion coefficient increased slightly with the increase in percentage of PET with values between  $11.3 \times 10^{-2} \text{ m}^2/\text{s}$  and  $16 \times 10^{-2} \text{ m}^2/\text{s}$  respect to the control sample of  $10.1 \times 10^{-2} \text{ m}^2/\text{s}$ . Samples values cured in the laboratory environment were higher than the samples values cured in the outdoor environment and the wet chamber.

As described in the literature, it is possible to improve some durability properties of RC when PET aggregates are incorporated into the mix. Likewise, various natural inhibitors have been reported to prevent the corrosion of RS. Therefore, the main objective of this research work is the study of the mechanical and durability properties of concrete. This project focuses on the use of nopal NM as a substitute for mixing-water and PET aggregates as a substitute for fine aggregate. Two elements were used for the study: mucilage obtained from a nopal-water ratio of 1-3 and PET (three geometries) with a substitution percentage of 3% in relation to the volume of the sand. The analysis was carried out through techniques such as:  $f'_c$ , HCP, EN, and LPR.

## 2. EXPERIMENTAL DESIGN.

### 2.1 Materials.

Composite Portland cement CPC-30R (Type II ASTM C-150) was used in this work. The coarse aggregate from crushed stone of local source was a maximum size of 20 mm, sand river was used as the fine aggregate and the steel rebars of grade 42 embedded in the concrete was a diameter of 10 mm.

### 2.2 Recycled PET geometric design.

The design of the different PET geometries was based on our previous studies (Díaz-Blanco et al. 2019). Waste PET bottles were collected and cleaned with water to eliminate all liquid, dust or grease residues. Once the containers were dried, the neck and bottom of the bottles were removed. The central part was cut into strips until the SF, LF and P of waste PET were obtained. For the SF, the dimensions were of 2-3 mm wide and 15 mm long, the LF were 0.5-1 mm wide and 25 mm long and the P were 3-4 mm wide and long. The entire procedure was carried out manually and easily.

### 2.3 NM extraction procedure.

To determine the concentration of NM, our previous studies were taken as a reference (Díaz Blanco et al. 2019). Fresh nopal leaves were collected and spines were removed. After, the leaves were washed to remove all kinds of residues or impurities and were cut into 1 cm x 1 cm pieces to finally be placed inside a beaker with water, in a nopal-water ratio of 1-3. The extraction of the NM was carried out by a maceration process at room temperature within the laboratory. After 48 hours, the solution was filtered to eliminate the nopal residues and proceed to use the mucilage as a substitute for the mixing water of the samples concrete.

### 2.4 Design of concrete mixtures.

The mix design was in accordance with the design resistance of  $250 \text{ kg}/\text{cm}^2$ . Therefore, the cement, the coarse and fine aggregate and the water were dosed according to Table 1. The PET aggregate was incorporated into the different mixtures as a partial substitute for the fine aggregate in a sand-PET volume ratio of 97%-3%. The inhibitor was added as a total substitute for the mixing water in all the samples containing the different PET geometries. For the control samples a water / cement

ratio of 0.45 was used. A mucilage/cement ratio was used in the case of samples with PET with the same value.

## 2.5 Specimens design.

### 2.5.1 Specimens for compressive resistance tests.

Cylindrical specimens were designed from PVC tubes with the following dimensions: 4.3 cm wide and 8.6 cm high with a height / diameter ratio equal 2, as represented in Figure 1. The requirements of the ASTM C-39 (C-39 2014) standard, and the Mexican NMX-C-083-ONNCCE standard were taken into account for each PET geometry and for the reference sample.



Figure 1. Representation of cylindrical specimens.

### 2.5.2 Samples for electrochemical tests.

For the electrochemical tests the design of the blocks was carried out leaving a concrete coverage of 3 cm (distance between the face of the steel bars and the edge of the specimens). The dimensions of the specimens were as follows: 7 cm wide, 10 high and 10 cm long. Three reinforcing steel bars embedded in the concrete with an exposed area (area in contact with the concrete matrix) of 18 cm<sup>2</sup> were placed. This is the standard method for the EN technique; the use of three nominally identical electrodes (Cottis 2001, 2008). The surface of each working electrode at the concrete-atmosphere interface was covered with an insulating tape. After 28 days of curing, they were partially submerged in a 3% sodium chloride solution simulating a marine environment such as seawater. A 2 cm difference was left between the level of the sodium chloride solution and the top of the blocks. Figure 2 shows the sample made for the electrochemical study.



Figure 2. Concrete block with three reinforcing steel bars.

The procedure for the elaboration of all cylindrical and blocks samples was very similar, as described in Figure 3.

1. All solid elements were mixed, including the addition of PET.
2. Once the water was incorporated in the case of the control samples and the NM inhibitor in the samples with PET aggregates, all the elements were mixed trying to obtain a mixture as homogeneous as possible. The whole process was carried out at room temperature.
3. Burnt oil was used to coat the molds of the samples and thus ensure that during the demolding, no fissures and cracks are formed, and that concrete blocks and cylinders do not fragment.
4. The pouring of the material was carried out in layers, compacting each layer until completing a total of two layers for each specimen.
5. Only in the case of the concrete blocks, the placement process of the bars, the pouring and compacting concrete was carried out simultaneously.
6. In the case of cylindrical specimens, the vertical and horizontal leveling of the samples was guaranteed. The upper surface of the samples was flattened, remaining smooth and free of imperfections.
7. After 24 hours, all samples were placed in a container with water for 28 days.

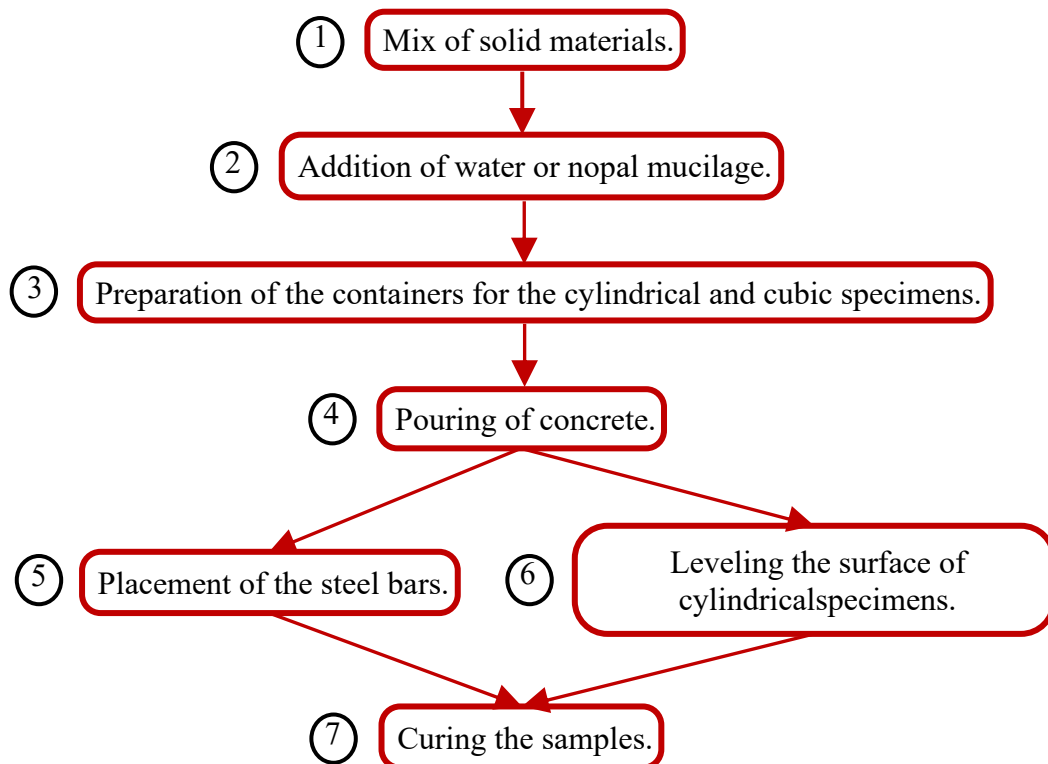


Figure 3. Schematic procedure followed for the elaboration of concrete samples.

Table 1 describes the characteristics and nomenclature of all the samples.

Table 1. Characteristics of the samples.

Samples	Type of aggregate (PET and NM)	Type of test	Nomenclature
1	No aggregates	Compressive strength	C-0
2	3% of P of PET and NM concentration of 1-3	Compressive strength	C-1
3	1.5 % of LF and 1.5% of P of PET, and NM concentration of 1-3	Compressive strength	C-2
4	3% of SF of PET and NM concentration of 1-3	Compressive strength	C-3
5	No aggregates	Electrochemical tests	E-0
6	3% of P of PET and NM concentration of 1-3	Electrochemical tests	E-1
7	1.5 % of LF and 1.5% of P of PET, and NM concentration of 1-3	Electrochemical tests	E-2
8	3% of SF of PET and NM concentration of 1-3	Electrochemical tests	E-3

## 2.6 Compressive strength technique.

The cylindrical samples were evaluated at 28 days of curing in a compression testing machine until reaching their maximum breaking load, according to the ASTM C-39 standard (C-39 2014). The specimens were placed aligning both axes with respect to the load axes of the equipment. The breaking load was recorded and from this, the strength of the concrete was determined by dividing the load by the sample section area, see equation 1:

$$f'_c = \frac{F}{A} \quad (1)$$

where:  $f'_c$ , is the compressive strength of concrete in  $\text{kg}/\text{cm}^2$ ;  $F$ , is the maximum breaking load registered by the equipment in kg and  $A$ , is the cross-sectional area of sample in  $\text{cm}^2$ .

## 2.7 Measurement of electrochemical techniques.

The HCP technique is a very simple and widely used tool for studying the corrosion of CRS (Kim et al. 2014; Leelalerkiet et al. 2004; Yodsudjai and Pattarakittam 2017). Although it has the limitation that it is not capable of providing information on the rate and corrosion mechanism (Ghorbani et al. 2019).  $E_{\text{corr}}$  readings were taken from the three bars of each sample and their average was recorded. Measurements were made with a saturated calomel electrode (SCE) as a reference electrode and a multimeter to record the values. From the HCP values and as established in the ASTM C876 (C876-09 2009) standard on the corrosion probability criterion, three intervals are established that relate both parameters. Zone 1 presents a 10% probability of corrosion in the range of values more positive than -125 mV; zone 2 covers a range of values between -125 mV to -276 mV (uncertainty zone); and zone 3 with a 90% probability of corrosion corresponds to the most negative range at -276 mV (Taji et al. 2018). As described by Cottis (Cottis 2001, 2008), the standard and most commonly used method for applying the EN technique is through the use of three nominally "identical" electrodes. Noise fluctuations in potential and current were simultaneously recorded for a time of 1024 s with a sampling frequency of 1 Hz. The results are from the three samples that contribute to the noise (tripled). For the analysis of the data obtained,

the trend removal of the current and potential time series was carried out by the linear regression method (Mansfeld, Sun, and Hsu 2001).

Many studies in reinforced concrete report the use of the LPR technique to study the corrosion of reinforcing steel (Clément et al. 2012; Samson et al. 2018). The results of this technique were obtained in triplicate and their value was averaged, which was represented in the graphs. In this investigation, a potential sweep of 30 mV was applied at a rate of 10 mV/min. Low-field polarization is non-intrusive, and values in the 10 to 30 mV range have been reported (Alghamdi and Ahmad 2014; Nguyen et al. 2018; Papavinasam 2008). From the slope formed by the applied potential values around the  $E_{corr}$  and the current response obtained, it is possible to determine the  $R_p$  (Zhou et al. 2018), as stated in the following equation (Mitzithra et al. 2015; Papavinasam 2008):

$$R_p \left( \frac{\Delta V}{\Delta I} \right)_{E_{corr}} \quad (2)$$

The design of the electrochemical cell for the study of RC is shown in Figure 4.

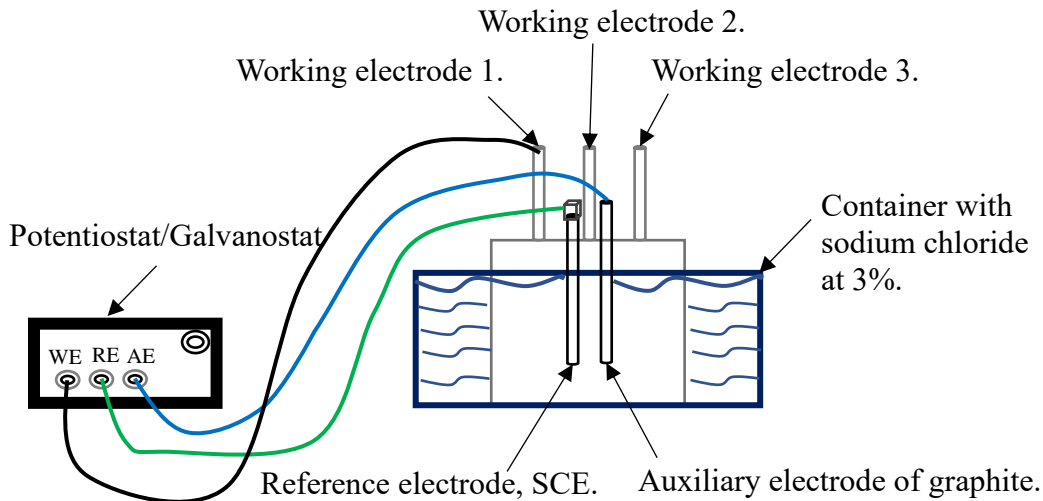


Figure 4. Representation of an electrochemical cell of RC for the LPR measurement.

### 2.8 Procedure to calculate corrosion rate.

The  $I_{corr}$  of the CRS was determined according to equation 3 (Nguyen et al. 2018; Zhou et al. 2018). In many investigation a B value of 26 mV has been used (Papavinasam 2008) and in this present paper research this same value will be considered for the calculation of  $I_{corr}$ .

$$I_{corr} = \frac{B}{R_p} \quad (3)$$

where:  $I_{corr}$ , is the corrosion rate in terms of the corrosion current density in  $\mu A/cm^2$ ; B, is the proportionality constant related to the Tafel slopes (anodic and cathodic), and  $R_p$ , is the polarization resistance.

Considering other previous studies in which the equivalence between the  $R_n$  and  $R_p$  values is demonstrated (Díaz Blanco et al. 2019), the  $I_{corr}$  values were determined from the  $R_n$  according to equation 3.

### 3. EXPERIMENTAL RESULTS.

#### 3.1. Compressive strength.

The Table 2 shows the average values of three samples for each PET geometry with NM compared to the control samples.

Table 2. Average values of  $f'_c$  at 28 days of curing.

Samples	$f'_c$ (kg/cm <sup>2</sup> )
C-0	248.9
C-1	231.1
C-2	238.5
C-3	233.0

As can be observed, the highest  $f'_c$  value for the samples with aggregates was achieved for sample C-2, with a value of 238.5 kg/cm<sup>2</sup>, primarily due to the effect of long fibers in the concrete matrix, which acts as a suppressor element in the formation and propagation of fissures and cracks (Foti 2013; Foti and Paparella 2014). Samples C-3 and C-1 follow in descending order of value, compared to the control sample with an average value of 248.9 kg/cm<sup>2</sup> relative to the design strength of 250 kg/cm<sup>2</sup>. These strength values are a consequence of the action of the NM, which acts as a cement setting retarder (Martínez-Barrios et al. 2025). The NM can retain water within the concrete, as the hydrophilic part of the polymers traps small water particles, slowing down the cement hydration process (Martínez-Barrios et al. 2025).

Furthermore, the good performance of the fibers can be seen in comparison with the shaped particles, where sample C-2 with 1.5% of LF and 1.5% of P achieved the highest resistance values compared to samples C-1 and C-3, which have 3% of P and 3% of SF, respectively. Several studies confirm the effect that PET fibers provide compared to other types of particles in terms of compression resistance properties (Bahij et al. 2020).

#### 3.2. Half-cell potential.

Previous studies showed that as the concentration of PET in its different geometries decreased, the protective effect of the steel became more significant in the long term (Díaz-Blanco et al. 2019; Díaz Blanco et al. 2019). The graph below illustrates the significant effect of decreasing the PET percentages and the effect of NM on the electrochemical properties of the reinforcing steel, see Figure 5.

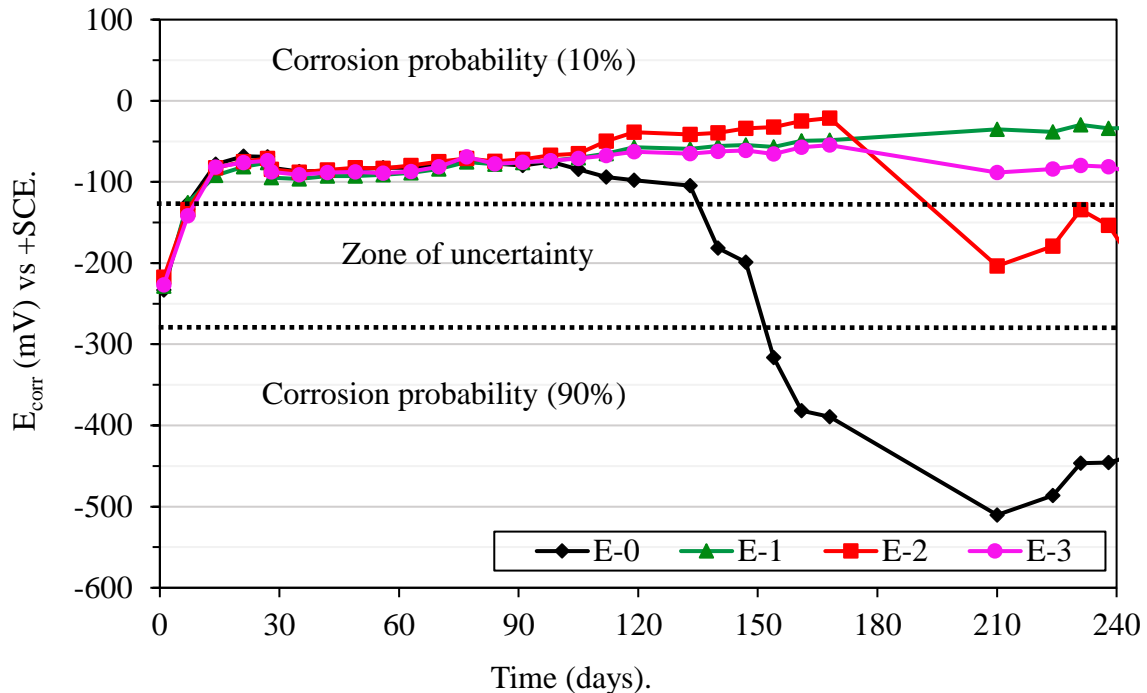


Figure 5.  $E_{\text{corr}}$  values for samples concrete exposed to 3% sodium chloride solution.

During the first 28 days of concrete setting, a sharp change in potential values towards more positive values is observed, related to the concrete curing process and the passivation of the reinforcing steel (Díaz-Blanco et al. 2019; Díaz Blanco et al. 2019). At these potential values, the reinforcing steel is completely passivated, falling into a zone with a 10% probability of corrosion. During the first three months of testing, all samples showed similar values. However, as the samples were exposed to the aggressive 3% sodium chloride solution for longer periods, the control sample (E-0) began to lose its protective properties and its  $E_{\text{corr}}$  values became more negative (Martínez-Barrios et al. 2025), reaching values of up to -500 mv after 210 days of exposure (90% probability of corrosion zone).

Furthermore, samples E-1 and E-3 remain in the 10% probability of corrosion zone for up to 240 days, demonstrating the positive effect of PET particles and short fibers as a physical barrier combined with NM on the electrochemical properties of concrete. The addition of NM partially blocks the pores within the concrete matrix, thus reducing the diffusion of aggressive agents (Pattusamy et al. 2023). Likewise, the mucilage of the prickly pear cactus retains moisture for a longer period of time. Different studies show that the polysaccharides present in the NM are hygroscopic, decreasing the loss of moisture from the material (Chandra, Eklund, and Villarreal 1998; Martínez-Barrios et al. 2025). Also, the effect of the NM act, decreasing the porosity of the material (Martínez-Barrios et al. 2025; Pattusamy et al. 2023) and act clogging pores stopping water and aggressive agents transport (chloride) into de concrete (Torres-Acosta and Alejandra Díaz-Cruz 2020).

Finally, sample E-2, which contains 1.5% long fibers and 1.5% particles, maintained acceptable behavior close to the uncertainty zone, but also maintained more positive values than sample E-0.

### 3.3. Electrochemical noise.

Using EN analysis, the standard deviation values of the current and the  $R_n$  values were determined. Figure 6 shows the results obtained by dividing the standard deviation of the noise voltage  $\sigma_v$  by the standard deviation of the noise current  $\sigma_i$ , resulting in the  $R_n$ .

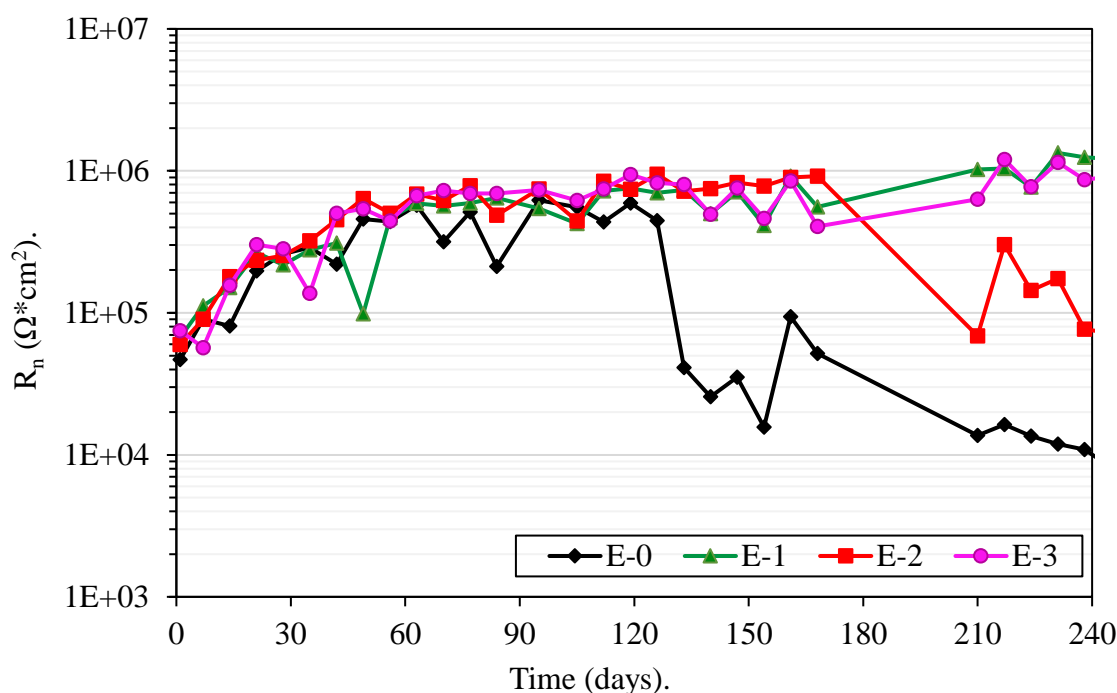


Figure 6.  $R_n$  values for samples concrete exposed to 3% sodium chloride solution.

During the first few months, the test specimens showed increasing  $R_n$ , related to the concrete curing process and the formation of a protective oxide film on the steel surface, exceeding  $500,000 \Omega^*cm^2$ . Between days 130 and 160, a sharp drop in  $R_n$  values was observed, mainly for sample E-1, with fluctuations throughout this period, demonstrating that the onset of active corrosion of the steel is not caused by a single change, but by a sequence of severe events. During this time, the remaining samples maintained very high  $R_n$  values close to  $750,000 \Omega^*cm^2$ , consistent with other previous studies (Díaz-Blanco et al. 2019; Díaz Blanco et al. 2019). Several studies have reported that NM acts as a pore clog in concrete, slowing down the penetration of chlorides through the concrete matrix by forming a chemical bond between the pectins and chloride/water molecules (Torres-Acosta 2007).

As the exposure time of the samples to the aggressive medium progresses, a drop in the  $R_n$  values for sample E-2 is observed, reaching approximately  $100,000 \Omega^*cm^2$ , remaining significantly higher than that of sample E-0. On the other hand, samples E-1 and E-3, which contain (3% PET particles plus nopal) and (3% short fibers plus nopal), respectively, maintain  $R_n$  values that reach up to  $1,000,000 \Omega^*cm^2$ . (Díaz Blanco et al. 2019) reported the effect of PET particles as a physical barrier within the concrete matrix, preventing the penetration of aggressive agents through the concrete's pore network. This effect is less pronounced in sample E-2, which contains (1.5% long fibers, 1.5% particles, and NM), thus confirming that the geometry of the PET has a significant effect on the electrochemical properties of concrete and on the protection of steel. The NM, for its part, had a significant effect on increasing the  $R_n$  values of all samples containing this corrosion inhibitor. This behavior supports the theory that NM inhibits the corrosion of reinforcing bars exposed to chloride aggressive medium (Torres-Acosta 2007).

### 3.4. Linear polarization resistance.

The results obtained from the LPR technique are shown in Figure 7. During the first three months of testing, a considerable increase in  $R_p$  was observed; these values are similar to the  $R_n$  values, associated with the formation of the passive steel layer within the concrete matrix. As the exposure time to the aggressive sodium chloride medium increased, there was a sharp drop in  $R_p$  values,

mainly for sample E-0 without inhibitor and without PET aggregates. The remaining samples maintained  $R_p$  values above  $100,000 \Omega \cdot \text{cm}^2$ , compared to sample E-0, whose values at the end of the test period barely exceeded  $30,000 \Omega \cdot \text{cm}^2$ . The inhibitory effect of the NM and the protective effect of the short fibers and particles (E-1 and E-3) are noteworthy, as their  $R_p$  values at several points reached values above  $1,000,000 \Omega \cdot \text{cm}^2$ .

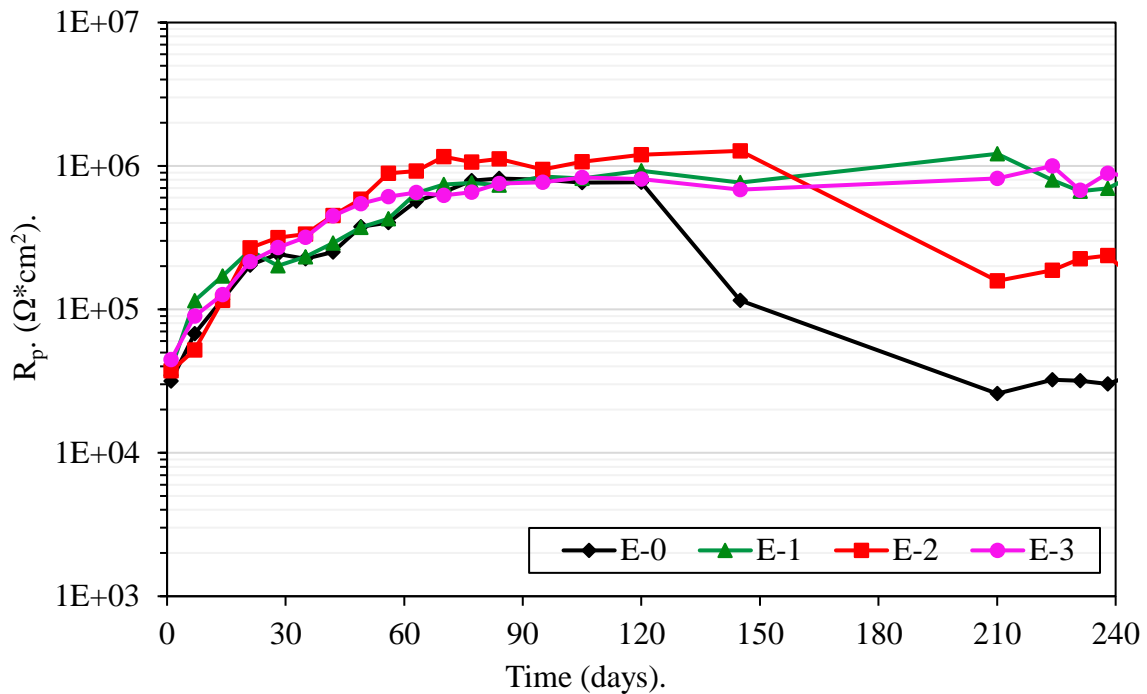


Figure 7.  $R_p$  values for concrete samples exposed to 3% sodium chloride solution.

According to ACI Committee 201 (ACI 2008), the formation of cracks and fissures in concrete can lead to an increase in the penetration rate of chloride ions, whereas the penetration rate of chlorides through diffusion is slower. In this sense, the introduction of PET fibers into concrete can act as a matrix reinforcement capable of restricting the formation of cracks and fissures. It can reduce the access of aggressive ions to the concrete and the initiation and propagation of corrosion.

Additionally, some properties of NM had a significant effect on these  $R_p$  values, such as viscosity, improving the workability and homogeneity of the mixture in the concrete (León-Martínez et al. 2014), decreasing the porosity of the concrete (Martínez-Barrios et al. 2025), and acting as a pore blocker (Pattusamy et al. 2023).

### 3.5. Corrosion rate.

Figure 8 and Figure 9 show the corrosion rate values of all concrete samples with and without inhibitor and PET aggregates.

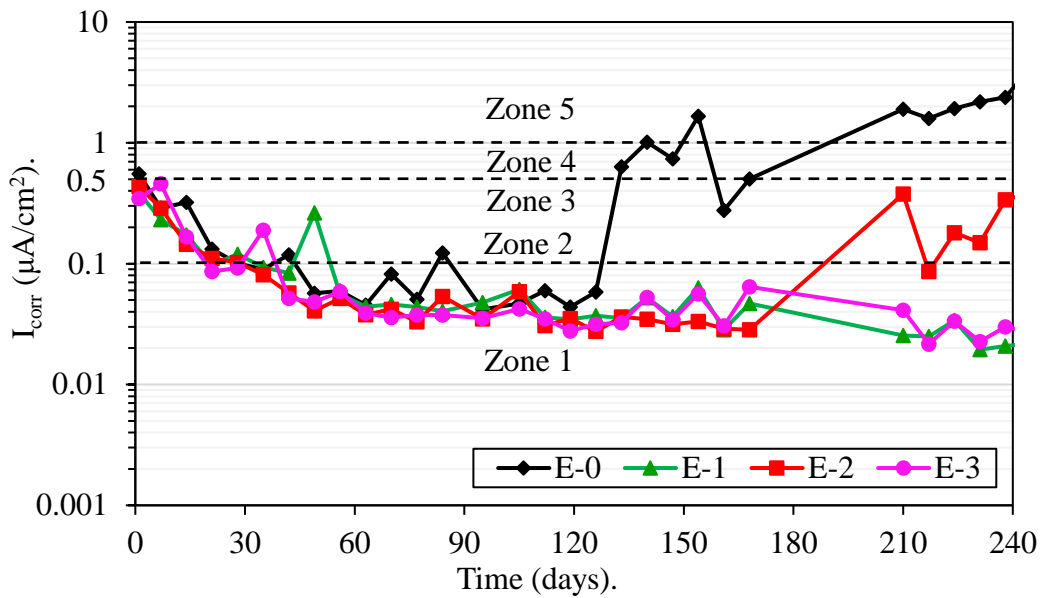


Figure 8.  $I_{corr}$  values from de  $R_n$  for concrete samples exposed to 3% sodium chloride solution.

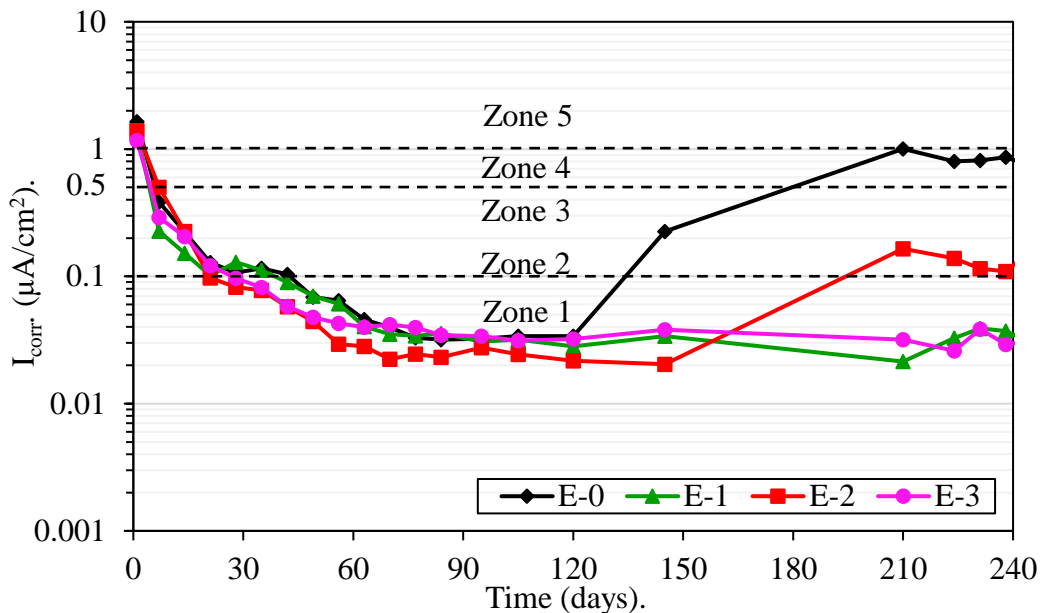


Figure 9.  $I_{corr}$  values from de  $R_p$  for concrete samples exposed to 3% sodium chloride solution.

At the beginning of the concrete curing stage, the samples exhibited corrosion rates ranging from very high (Zone 5) to high (Zone 4). During this initial phase, all the concrete components reacted with the water and added NM to form the various compounds that gave the concrete its alkalinity, strength, and durability. At the end of this 28-day curing process, the  $I_{corr}$  values decreased by an order of magnitude, approaching zones 1 and 2, which are characterized by negligible and low corrosion rates. In this range, steel possibly already developed a state of passivity due to the presence of moisture, oxygen and a highly alkaline medium (Hansson 1984).

At the end of the testing period, it was observed that samples E-1 and E-3 maintained very low  $I_{corr}$  values in zone 1, which is related to the passivity of the steel for a longer period of time. Both the NM and (SF and P of PET) provided the concrete with double protection, preventing chloride ions

from reaching the steel and maintaining stable factors such as humidity, oxygen, and alkalinity of the concrete for a longer period.

In both graphs, a similarity can be seen in terms of the results achieved, maintaining the same trend over time.

### 3.6. Visual observation of the steel bars.

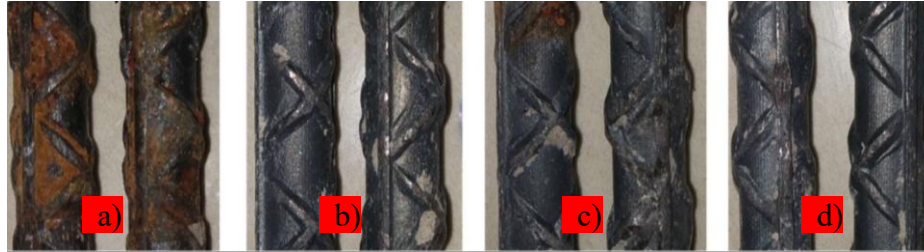


Figure 10. Steel rods extracted from concrete after 240 days of exposure to a 3% sodium chloride solution: a) sample E-0, b) sample E-1, c) sample E-2 and d) sample E-3.

As shown in Figure 10, reddish corrosion products are visible on more than 80% of the metal surface in sample E-0. In contrast, this chloride ion attack, with subsequent depassivation of the steel and loss of its protective properties, was less pronounced in the remaining samples, primarily in samples E-1 and E-3, which exhibit a metallic gray tone across the entire steel surface. In the case of sample E-2, which presents NM and (1.5% LF-PET and 1.5% P-PET), only some small areas of rust are observed, which appear as smaller corrosion zones.

## 4. CONCLUSIONS.

Based on the analysis of the electrochemical and mechanical behavior results of concrete with the addition of PET and NM, the conclusions are the following:

All samples C-1, C-2, and C-3 achieved adequate  $f'_c$  values considering the percentages of PET and geometries used and the concentration of NM. Sample C-2, in particular, with the addition of LF plus P, achieved the value closest to that of the control sample C-O.

In general, all samples with NM inhibitor and PET aggregates maintained less negative  $E_{corr}$  values than the control sample (E-0), keeping the steel in a passive state for a longer period. The effect of PET as a physical barrier and some properties of NM, such as its viscosity and composition, gave the concrete greater durability against aggressive agents such as chloride ions.

The  $R_n$  and  $R_p$  values showed a similar trend between the two results. These results support the use of both techniques to evaluate the corrosion behavior of steel embedded in concrete. Samples E-1 and E-3 showed the highest  $R_n$  and  $R_p$  values, which supports the good performance of the designed composite material.

The  $I_{corr}$  maintained very negligible corrosion rate values for all samples with aggregates and the steel bars extracted from the samples, visually reflecting the protective effect of both compounds (PET and NM).

## 5. ACKNOWLEDGEMENTS.

This work was supported by a postdoctoral fellowship from the Secretaria de Educación, Ciencia, Humanidades, Tecnología e Innovación (SECIHTI)/Consejo Nacional de Humanidades, Ciencia, y Tecnología (CONAHCYT), México.

## 6. REFERENCES.

- El Fattah, A. A., Al-Duais, I., Riding, K., and Thomas, M. (2018), “*Field Evaluation of Corrosion Mitigation on Reinforced Concrete in Marine Exposure Conditions*”. *Construction and Building Materials*. 165:663–74. <https://doi.org/10.1016/j.conbuildmat.2018.01.077>.
- Abdel-Gaber, A. M., Khamis, E., and Hefnawy, A. (2011), “*Utilizing Arghel Extract as Corrosion Inhibitor for Reinforced Steel in Concrete*”. *Materials and Corrosion*. 62(12):1159–1162. <https://doi.org/10.1002/maco.201005653>.
- ACI. (2008). “*Guide to Durable Concrete Reported*”. ACI Committee 201 1–41.
- Adnan, H. M., and Dawood, A. O., (2020), “*Strength Behavior of Reinforced Concrete Beam Using Re-Cycle of PET Wastes as Synthetic Fibers.*” *Case Studies in Construction Materials*. 13:1-19. <https://doi.org/10.1016/j.cscm.2020.e00367>.
- Alfahdawi, I. H., Osman, S. A., Hamid, R., and AL-Hadithi, A. I. (2019), “*Influence of PET Wastes on the Environment and High Strength Concrete Properties Exposed to High Temperatures.*” *Construction and Building Materials*. 225:358–370. <https://doi.org/10.1016/j.conbuildmat.2019.07.214>.
- Alghamdi, S. A., and Ahmad, S. (2014), “*Service Life Prediction of RC Structures Based on Correlation between Electrochemical and Gravimetric Reinforcement Corrosion Rates.*” *Cement and Concrete Composites*. 47:64–68. <https://doi.org/10.1016/j.cemconcomp.2013.06.003>.
- Andrade, C., Alonso, C., and Sarra, J. (2002), “*Corrosion Rate Evolution in Concrete Structures Exposed to the Atmosphere.*” *Cement and Concrete Composites*. 24(1):55–64. [https://doi.org/10.1016/S0958-9465\(01\)00026-9](https://doi.org/10.1016/S0958-9465(01)00026-9).
- Sifatullah, B. Omary, S. Feugeas, F. and Faqiri, A. (2020), “*Fresh and Hardened Properties of Concrete Containing Different Forms of Plastic Waste – A Review.*” *Waste Management*. 113:157–75. <https://doi.org/10.1016/j.wasman.2020.05.048>.
- Borg, R. P., Baldacchino, O. and Ferrara, L. (2016), “*Early Age Performance and Mechanical Characteristics of Recycled PET Fibre Reinforced Concrete.*” *Construction and Building Materials*. 108:29–47. <https://doi.org/10.1016/j.conbuildmat.2016.01.029>.
- ASTM International (20214). *ASTM C-39, Standard Test Method for Compressive Strength of Cylindrical Concrete Specimens*. [https://doi.org/10.1520/C0039\\_C0039M-14](https://doi.org/10.1520/C0039_C0039M-14)
- ASTM International (2009). *ASTM C876-09, “Standard Test Method for Corrosion Potentials of Uncoated Reinforcing Steel in Concrete.”* ASTM International. 1–7. <https://doi.org/10.1520/C0876-09>.
- Chandra, S., L. Eklund, L., and Villarreal, R. R. (1998), “*Use of Cactus in Mortars and Concrete.*” *Cement and Concrete Research*. 28(1):41-51. [https://doi.org/10.1016/S0008-8846\(97\)00254-8](https://doi.org/10.1016/S0008-8846(97)00254-8)
- Clément, A., Laurens, S., Arliguie, G., and Deby, F. (2012), “*Numerical Study of the Linear Polarisation Resistance Technique Applied to Reinforced Concrete for Corrosion Assessment.*” *European Journal of Environmental and Civil Engineering*. 16(3–4):491–504. <https://doi.org/10.1080/19648189.2012.668012>.
- Cottis, R. A. (2001), “*Interpretation of Electrochemical Noise Data.*” *Corrosion*. 57(3):265–285. <https://doi.org/10.5006/1.3290350>
- Cottis, R. A. (2008), “*Electrochemical Noise for Corrosion Monitoring.*” Pp. 86–110 in *Techniques for Corrosion Monitoring*, Elsevier. <https://doi.org/10.1016/B978-0-08-103003-5.00005-9>
- Díaz-Blanco, Y., Menchaca-Campos, E. C., Rocabrano-Valdés, C. I., and Uruchurtu-Chavarín, J. (2019), “*Effect of Recycled PET (Polyethylene Terephthalate) on the Electrochemical Properties of Rebar in Concrete.*” *International Journal of Civil Engineering*. 18:487–500. <https://doi.org/10.1007/s40999-019-00478-3>.

- Díaz-Blanco, Y., Menchaca Campos E. C., Rocabruno-Valdés, C. I., and Uruchurtu-Chavarín, J. 2019. “*Natural Additive (Nopal Mucilage) on the Electrochemical Properties of Concrete Reinforcing Steel.*” *Revista ALCONPAT*. 9(3):260–276. <https://doi.org/10.21041/ra.v9i3.429>.
- Foti, D. (2013), “*Use of Recycled Waste Pet Bottles Fibers for the Reinforcement of Concrete.*” *Composite Structures*. 96:396–404. <https://doi.org/10.1016/j.compstruct.2012.09.019>.
- Foti, D. (2019), “*Recycled Waste PET for Sustainable Fiber-Reinforced Concrete.*” Pp. 387–410 in *Use of Recycled Plastics in Eco-efficient Concrete*, Elsevier. <https://doi.org/10.1016/B978-0-08-102676-2.00018-9>
- Foti, D., and Paparella, F. (2014), “*Impact Behavior of Structural Elements in Concrete Reinforced with PET Grids.*” *Mechanics Research Communications*. 57:57–66. <https://doi.org/10.1016/j.mechrescom.2014.02.007>.
- Garcés, P., Saura, P. Méndez, A. Zornoza, E. and Andrade, C. (2008), “*Effect of Nitrite in Corrosion of Reinforcing Steel in Neutral and Acid Solutions Simulating the Electrolytic Environments of Micropores of Concrete in the Propagation Period.*” *Corrosion Science*. 50(2):498–509. <https://doi.org/10.1016/j.corsci.2007.08.016>.
- Nina, G. Kosec, T., and Legat, A. (2016), “*The Efficiency of a Corrosion Inhibitor on Steel in a Simulated Concrete Environment.*” *Materials Chemistry and Physics*. 184:31–40. <https://doi.org/10.1016/j.matchemphys.2016.08.047>.
- Ghorbani, S., Taji, I., Brito, J. D. Negahban, M., Ghorbani, S., Tavakkolizadeh, M., and Davoodi, A. (2019), “*Mechanical and Durability Behaviour of Concrete with Granite Waste Dust as Partial Cement Replacement under Adverse Exposure Conditions.*” *Construction and Building Materials*. 194:143–52. <https://doi.org/10.1016/j.conbuildmat.2018.11.023>.
- Hansson, C. M. (1984), “*Comments on Electrochemical Measurements of the Rate of Corrosion of Steel in Concrete.*” *Cement and Concrete Research*. 14(4):574–84. [https://doi.org/10.1016/0008-8846\(84\)90135-2](https://doi.org/10.1016/0008-8846(84)90135-2).
- Ben Harb, M., Abubshait, S., Etteyeb, N., Kamoun, M., and Dhouib, A. (2020), “*Olive Leaf Extract as a Green Corrosion Inhibitor of Reinforced Concrete Contaminated with Seawater.*” *Arabian Journal of Chemistry*. 13:4846–56. <https://doi.org/10.1016/j.arabjc.2020.01.016>.
- Kim, Y.Y., Kim, J. M., Bang, J. W., and Kwon, S. J. (2014), “*Effect of Cover Depth, w/c Ratio, and Crack Width on Half Cell Potential in Cracked Concrete Exposed to Salt Sprayed Condition.*” *Construction and Building Materials*. 54:636–45. <https://doi.org/10.1016/j.conbuildmat.2014.01.009>.
- Han-Seung L., Hyun-Min Y., Singh, J. K., Prasad, S. K., and Yoo, B. (2018), “*Corrosion Mitigation of Steel Rebars in Chloride Contaminated Concrete Pore Solution Using Inhibitor: An Electrochemical Investigation.*” *Construction and Building Materials*. 173:443–51. <https://doi.org/10.1016/j.conbuildmat.2018.04.069>.
- Leelalerkiet, V., Je-Woon K., Ohtsu, M. and Yokota, M. (2004), “*Analysis of Half-Cell Potential Measurement for Corrosion of Reinforced Concrete.*” *Construction and Building Materials*. 18:155–62. <https://doi.org/10.1016/j.conbuildmat.2003.10.004>.
- León-Martínez, F. M., Cano-Barrita, P. F. de J., Lagunez-Rivera, L., and Medina-Torres, L. (2014), “*Study of Nopal Mucilage and Marine Brown Algae Extract as Viscosity-Enhancing Admixtures for Cement Based Materials.*” *Construction and Building Materials*. 53:190–202. <https://doi.org/10.1016/j.conbuildmat.2013.11.068>.
- Liu, Y., Song, Z., Wang, W., Jiang, L., Zhang, Y., Guo, M., Song, F., and Xu, N. (2019), “*Effect of Ginger Extract as Green Inhibitor on Chloride-Induced Corrosion of Carbon Steel in Simulated Concrete Pore Solutions.*” *Journal of Cleaner Production*. 214:298–307. <https://doi.org/10.1016/j.jclepro.2018.12.299>.
- Loto, C. A., Joseph, O. O., Loto, R. T., and Popoola, A. P. I. (2013), “*Inhibition Effect of Vernonia Amygdalina Extract on the Corrosion of Mild Steel Reinforcement in Concrete in 3.5M NaCl*

- Environment.*” International Journal of Electrochemical Science. 8(9):11087–11100. [https://doi.org/10.1016/S1452-3981\(23\)13171-3](https://doi.org/10.1016/S1452-3981(23)13171-3)
- Mansfeld, F., Sun, Z. and Hsu, C. H. (2001), “*Electrochemical Noise Analysis (ENA) for Active and Passive Systems in Chloride Media.*” *Electrochimica Acta.* 46(24-25):3651–3664. [https://doi.org/10.1016/S0013-4686\(01\)00643-0](https://doi.org/10.1016/S0013-4686(01)00643-0).
- Martínez-Barrios, E., Páramo-García, U. Suárez-Domínguez, E. J., and Pérez-Sánchez, J. F. (2025), “*The Effect of Nopal Mucilage Addition on the Corrosion Rate of Reinforcement Steel in Concrete.*” *Surfaces* 8(26):1-12. <https://doi.org/10.3390/surfaces8020026>.
- Martinez-Molina, W., Torres-Acosta, A., Hernández-Leos, R., Alonso-Guzman, E., Mendoza-Pérez, I., and Martinez-Peña, I. (2016), “*The Inhibitive Properties of Nopal Slime on the Corrosion of Steel in Chloride-Contaminated Mortar.*” *Anti-Corrosion Methods and Materials.* 63(1):65–71. <https://doi.org/10.1108/ACMM-05-2014-1381>.
- Mitzithra, M. E., Deby, F. Balayssac, J. P., and Salin, J. (2015), “*Proposal for an Alternative Operative Method for Determination of Polarisation Resistance for the Quantitative Evaluation of Corrosion of Reinforcing Steel in Concrete Cooling Towers.*” *Nuclear Engineering and Design* 288:42–55. <https://doi.org/10.1016/j.nucengdes.2015.03.018>.
- Monticelli, C. (2018), “*Corrosion Inhibitors.*” Pp. 164–71 in *Encyclopedia of Interfacial Chemistry: Surface Science and Electrochemistry*, Elsevier. <https://doi.org/10.1016/B978-0-12-409547-2.13443-2>
- Nguyen, W., Duncan, J. F., Devine, T. M., and Ostertag, C. P. (2018), “*Electrochemical Polarization and Impedance of Reinforced Concrete and Hybrid Fiber-Reinforced Concrete under Cracked Matrix Conditions.*” *Electrochimica Acta.* 271:319–336 <https://doi.org/10.1016/j.electacta.2018.03.134>.
- Noroozi, R., Shafabakhsh, G. Kheyroddin, A. and Moghaddam, A. M. (2019), “*Investigating the Effects of Recycled PET Particles, Shredded Recycled Steel Fibers and Metakaolin Powder on the Properties of RCCP.*” *Construction and Building Materials.* 224:173–87. <https://doi.org/10.1016/j.conbuildmat.2019.07.012>.
- Okeniyi, J. O., Akintoye Loto, C. and Idowu Popoola, A. P. (2015), “*Investigating the Corrosion Mechanism of Morinda Lucida Leaf Extract Admixtures on Concrete Steel Rebar in Saline/Marine Simulating Environment.*” *International Journal of Electrochemical Science.* 10:9893–9906. [https://doi.org/10.1016/S1452-3981\(23\)11228-4](https://doi.org/10.1016/S1452-3981(23)11228-4)
- Okeniyi, J. O., Akintoye Loto, C., and Idowu Popoola, A. P. (2015), “*Corrosion Inhibition of Concrete Steel-Reinforcement in Saline/Marine Simulating-Environment by Rhizophora Mangle L.*” *Solid State Phenomena.* 227:185–189. <https://doi.org/10.4028/www.scientific.net/SSP.227.185>.
- Ongpeng, J. C. C., Barra, J., Carampatana, C., Sebastian, C., Yu, J. J. Aviso, K. B., and Tan, R. R. (2020). “*Strengthening Rectangular Columns Using Recycled PET Bottle Strips.*” *Engineering Science and Technology, an International Journal.* 24(2):405-413. <https://doi.org/10.1016/j.jestch.2020.07.006>.
- Ormellese, M., Berra, M. Bolzoni, F. and Pastore, T. (2006), “*Corrosion Inhibitors for Chlorides Induced Corrosion in Reinforced Concrete Structures.*” *Cement and Concrete Research* 36(3):536–47. <https://doi.org/10.1016/j.cemconres.2005.11.007>.
- Palanisamy, S. P., Maheswaran, G. Kamal, C. and Venkatesh, G. (2016), “*Prosopis Juliflora—A Green Corrosion Inhibitor for Reinforced Steel in Concrete.*” *Research on Chemical Intermediates* 42(12):7823–40. <https://doi.org/10.1007/s11164-016-2564-1>.
- Palanisamy, S. P., Maheswaran, G. Selvarani, A G., Kamal, C. and Venkatesh, G. (2018), “*Ricinus Communis – A Green Extract for the Improvement of Anti-Corrosion and Mechanical Properties of Reinforcing Steel in Concrete in Chloride Media.*” *Journal of Building Engineering.* 19:376–383. <https://doi.org/10.1016/j.jobe.2018.05.020>.

- Pan, C., Chen, N., He, J., Liu, S., Chen, K., Wang, P., and Xu, P. (2020), “*Effects of Corrosion Inhibitor and Functional Components on the Electrochemical and Mechanical Properties of Concrete Subject to Chloride Environment.*” *Construction and Building Materials* 260:119724. <https://doi.org/10.1016/j.conbuildmat.2020.119724>.
- Papavinasam, S. (2008), “*Electrochemical Polarization Techniques for Corrosion Monitoring.*” Pp. 45–77 in *Techniques for Corrosion Monitoring*, WP.. <https://doi.org/10.1016/B978-0-08-103003-5.00003-5>
- Pattusamy, L., Rajendran, M. Shanmugamoorthy, S. and Ravikumar, K. (2023), “*Confinement Effectiveness of 2900psi Concrete Using the Extract Euphorbia Tortilis Cactus as a Natural Additive.*” *Revista Materia*. 28(1). <https://doi.org/10.1590/1517-7076-RMAT-2022-0233>.
- Pradipta, I., Kong, D. and Lee Tan, J. B. (2019), “*Natural Organic Antioxidants from Green Tea Inhibit Corrosion of Steel Reinforcing Bars Embedded in Mortar.*” *Construction and Building Materials*. 227(10):117058. <https://doi.org/10.1016/j.conbuildmat.2019.117058>.
- Qian, S., and Cusson, D. (2004), “*Electrochemical Evaluation of the Performance of Corrosion-Inhibiting Systems in Concrete Bridges.*” *Cement and Concrete Composites*. 26(3):217–33. [https://doi.org/10.1016/S0958-9465\(03\)00041-6](https://doi.org/10.1016/S0958-9465(03)00041-6).
- Rahmani, E., Dehestani, M., Beygi, M. H. A., Allahyari, H., and Nikbin, I. M. (2013), “*On the Mechanical Properties of Concrete Containing Waste PET Particles.*” *Construction and Building Materials*. 47:1302–1308. <https://doi.org/10.1016/j.conbuildmat.2013.06.041>.
- Raja, P. B., Seyedmojtaba G., and Mohammad I. (2015), “*Natural Corrosion Inhibitors for Steel Reinforcement in Concrete — A Review.*” *Surface Review and Letters*. 22(3). <https://doi.org/10.1142/S0218625X15500407>.
- Sadmomtazi, A., Dolati-Milehsara, S., Lotfi-Omran, O., and Sadeghi-Nik, A. (2015), “*The Combined Effects of Waste Polyethylene Terephthalate (PET) Particles and Pozzolanic Materials on the Properties of Self-Compacting Concrete.*” *Journal of Cleaner Production*. 112(4):2363–2373. <https://doi.org/10.1016/j.jclepro.2015.09.107>.
- Saikia, N., and de Brito, J. (2014), “*Mechanical Properties and Abrasion Behaviour of Concrete Containing Shredded PET Bottle Waste as a Partial Substitution of Natural Aggregate.*” *Construction and Building Materials*. 52:236–244. <https://doi.org/10.1016/j.conbuildmat.2013.11.049>.
- Samson, G., Deby, F. Garcia, J. L., and Perrin, J. L. (2018), “*Alternative Methodology for Linear Polarization Resistance Assessment of Reinforced Concrete Structure.*” *MATEC Web of Conferences* 199. <https://doi.org/10.1051/mateconf/201819906009>.
- Saricimen, H., Mohammad, M., Quddus, A., Shameem, M., and Barry, M. S. (2002), “*Effectiveness of Concrete Inhibitors in Retarding Rebar Corrosion.*” *Cement and Concrete Composites*. 24:89–100. [https://doi.org/10.1016/S0958-9465\(01\)00030-0](https://doi.org/10.1016/S0958-9465(01)00030-0).
- De Schutter, G., and Luo, L. (2004), “*Effect of Corrosion Inhibiting Admixtures on Concrete Properties.*” *Construction and Building Materials*. 18:483–89. <https://doi.org/10.1016/j.conbuildmat.2004.04.001>.
- Siddique, R., Khatib, J. and Kaur, I. (2008), “*Use of Recycled Plastic in Concrete: A Review.*” *Waste Management*. 28(10):1835–52. <https://doi.org/10.1016/j.wasman.2007.09.011>.
- Silva, R. V., de Brito, J. and Saikia, N. (2013), “*Influence of Curing Conditions on the Durability-Related Performance of Concrete Made with Selected Plastic Waste Aggregates.*” *Cement and Concrete Composites*. 35:23–31. <https://doi.org/10.1016/j.cemconcomp.2012.08.017>.
- Taji, I., Ghorbani, S. de Brito, J. Tam, V. W. Y., Sharifi, S. Davoodi, A. and Tavakkolizadeh, M. (2018), “*Application of Statistical Analysis to Evaluate the Corrosion Resistance of Steel Rebars Embedded in Concrete with Marble and Granite Waste Dust.*” *Journal of Cleaner Production*. 210:837-846. <https://doi.org/10.1016/j.jclepro.2018.11.091>.

- Thomas, L. M., and Moosvi, S. A. (2020), “*Hardened Properties of Binary Cement Concrete with Recycled PET Bottle Fiber: An Experimental Study.*” *Materials Today: Proceedings.* 32(4):632-637. <https://doi.org/10.1016/j.matpr.2020.03.025>.
- Torres-Acosta, A. A. (2007), “*Opuntia-Ficus-Indica (Nopal) Mucilage as a Steel Corrosion Inhibitor in Alkaline Media.*” *Journal of Applied Electrochemistry.* 37(7):835–41. <https://doi.org/10.1007/s10800-007-9319-z>.
- Torres-Acosta, A. A., and Díaz-Cruz, L. A. (2020), “*Concrete Durability Enhancement from Nopal (Opuntia Ficus-Indica) Additions.*” *Construction and Building Materials.* 243:118170. <https://doi.org/10.1016/j.conbuildmat.2020.118170>.
- Umoren, S. A., Solomon, M. M., Obot, I. B., and Suleiman, R. K. (2019), “*A Critical Review on the Recent Studies on Plant Biomaterials as Corrosion Inhibitors for Industrial Metals.*” *Journal of Industrial and Engineering Chemistry.* 76:91–115. <https://doi.org/10.1016/j.jiec.2019.03.057>.
- Valipour, M., Shekarchi, M., and Ghods, P. (2014), “*Comparative Studies of Experimental and Numerical Techniques in Measurement of Corrosion Rate and Time-to-Corrosion-Initiation of Rebar in Concrete in Marine Environments.*” *Cement and Concrete Composites.* 48:98–107. <https://doi.org/10.1016/j.cemconcomp.2013.11.001>.
- Jong-Pil, W., Chang-Il J., Sang-Woo L., Su-Jin L., and Heung-Youl K. (2010), “*Long-Term Performance of Recycled PET Fibre-Reinforced Cement Composites.*” *Construction and Building Materials.* 24:660–665. <https://doi.org/10.1016/j.conbuildmat.2009.11.003>.
- Xu, J. X., Gao, G. F., Jiang, L. H., and Pang, D P. (2015), “*Corrosion Protection of Reinforcing Steel with Kelp Extract as Corrosion Inhibitor.*” *Materials Research Innovations.* 19(sup1): S1-20-S1-25. <https://doi.org/10.1179/1432891715Z.0000000001361>.
- Yodsudjai, W., and Pattarakittam, T. (2017), “*Factors Influencing Half-Cell Potential Measurement and Its Relationship with Corrosion Level.*” *Measurement: Journal of the International Measurement Confederation.* 104:159–68. <https://doi.org/10.1016/j.measurement.2017.03.027>.
- Zhang, Z., Ba, H. and Wu, Z. (2019), “*Sustainable Corrosion Inhibitor for Steel in Simulated Concrete Pore Solution by Maize Gluten Meal Extract: Electrochemical and Adsorption Behavior Studies.*” *Construction and Building Materials.* 227:117080. <https://doi.org/10.1016/j.conbuildmat.2019.117080>.
- Zhou, B., Gu, X., Guo, H., Zhang, W., and Huang, Q. (2018), “*Polarization Behavior of Activated Reinforcing Steel Bars in Concrete under Chloride Environments.*” *Construction and Building Materials.* 164:877–887. <https://doi.org/10.1016/j.conbuildmat.2018.01.187>.